

**THE GAO-GUENIE (BURKINA FASO) IMPACT MELT BRECCIA – A PIECE OF AN IMPACT MELT INJECTION DIKE ON AN H-CHONDRITE ASTEROID.** Martin Schmieder<sup>1,2</sup>, David A. Kring<sup>1,2</sup>, Timothy D. Swindle<sup>3,2</sup>, Jade C. Carter-Bond<sup>4</sup>, and Carleton B. Moore<sup>5</sup>, <sup>1</sup>Lunar and Planetary Institute, 3600 Bay Area Boulevard, Houston, TX 77058, USA, schmieder@lpi.usra.edu, <sup>2</sup>NASA Solar System Exploration Research Virtual Institute, <sup>3</sup>Lunar and Planetary Laboratory, University of Arizona, 1629 East University Boulevard, Tucson, AZ 85721, USA, <sup>4</sup>Department of Astrophysics, School of Physics, University of New South Wales, Sydney NSW 2052, Australia, <sup>5</sup>Center for Meteorite Studies, Arizona State University, Tempe, AZ 85287, USA.

**Introduction:** The Gao-Guenie meteorite, an H5 chondrite that fell in Burkina Faso in March 1960 [1,2], has portions that were impact-melted on the H-chondrite parent body at ~300 Ma [3]. Fragments of this asteroidal impact melt breccia were, through later impact events in space (see [4,5]), sent into an Earth-crossing orbit. A new petrographic–geochemical study of the shocked and impact-melted domains of the Gao-Guenie impact melt breccia (GGIMB) provides insights into the shock conditions during melt formation and post-shock cooling of the melt body. A determination of cooling rates puts additional constraints on the geologic setting where the GGIMB was produced on the H-chondrite parent body (compare [6]).

**Samples and Analytical Techniques:** A polished thin section of the GGIMB (sample LPL 1055,1; ~4.2 cm<sup>2</sup>) was analyzed using an optical microscope and its modal composition quantified in a point count (n=5,319). Geochemical analyses were done using a CAMECA SX-100 electron microprobe at the NASA Johnson Space Center (operated at 15 kV; 1 μm beam diameter; 10 nA for silicates, 20 nA for metals; and a set of well-characterized mineral and metal standards).

**Petrography and Geochemistry:** Sample LPL 1055,1 (Fig. 1a) consists of a coarser-crystalline chondrite-clast domain (~29%), a micro- to crypto-crystalline quench melt/vein domain adjacent to clasts (~18%), and an igneous-textured, microporphyritic, impact melt-matrix domain (~53%). The impact melt domain (Fig. 1b) contains ~84% silicates (~4% of which are relic grains inherited from the shocked chondrite target), ~7% Fe,Ni metal, and ~5% sulfide (troilite). Relic olivine in the impact melt domain commonly exhibits planar fractures and shock darkening, as well as internal recrystallization features consistent with the formation of a whole-rock melt at peak shock pressures of ~75–90 GPa and post-shock temperatures ≥1,500°C [7]. Whereas metal–troilite aggregates in the clast domain show textural evidence for incipient melting, the impact melt domain has abundant once-molten metal–troilite droplets (Fig. 1c) up to ~2 mm in diameter. Chromite and apatite occur as accessory minerals. No ringwoodite was found.

The composition of olivine is relatively homogeneous across the GGIMB (Fo<sub>80–82</sub>). Pyroxene in the clast domain is low-Ca pyroxene (Wo<sub>1–3</sub>En<sub>83–81</sub>Fs<sub>18–16</sub>).

Melt-grown pyroxene crystals in the impact melt domain are commonly zoned, with low-Ca pyroxene cores surrounded by pigeonite (Wo<sub>6–14</sub>En<sub>77–70</sub>Fs<sub>17</sub>) and augite (Wo<sub>23</sub>En<sub>63</sub>Fs<sub>14</sub>) rims. Chromite in the clast and melt domain is Chr<sub>84–85</sub>Hc<sub>16–15</sub>. The cores of Fe,Ni-metal orbs in the impact melt domain (martensite?) contain an average of ~7.8 wt% Ni, ~0.5 wt% Co and ~0.4 wt% P (n=525 beam spots in 20 line scans), and are typically surrounded by taenite (with an average of ~11.7 wt%, and up to ~18 wt% Ni) and Ni-bearing troilite (~0.26 wt% Ni on average).

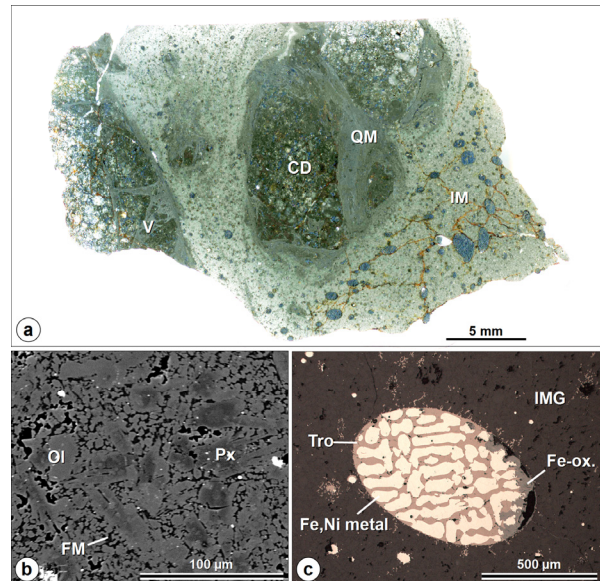


**Fig. 1:** The Gao-Guenie impact melt breccia (sample LPL 1055,1). (a) Scan of polished thin section, showing clast domain (CD), veins (V), larger domains of quench melt (QM), and impact melt domain (IM) with several larger metal–troilite orbs visible. (b) Backscattered electron image of the igneous-textured, microporphyritic, impact melt domain, with melt-grown olivine (Ol), pyroxene (Px), and a feldspathic mesostasis (FM). (c) Reflected light photomicrograph of a typical Fe,Ni metal–troilite (Tro) orb in the impact melt groundmass (IMG). The orb has been partially altered to secondary Fe-oxides (Fe-ox.) along its rim.

**Estimated Cooling Rates:** Impact melt breccias have a characteristic two-stage cooling profile; stage I cooling involves the thermal equilibration of the superheated impact melt with relatively cold clasts, while stage II cooling represents the (usually conductive) cooling of the melt breccia to its colder surround-

ings. Following the methods and equation of [8], a metallographic analysis of the width (37–46  $\mu\text{m}$ ;  $n=160$ ) and spacing (52–62  $\mu\text{m}$ ;  $n=136$ ) of subparallel Fe,Ni-metal cells in 9 representative metal–troilite orbs indicate a stage I cooling rate of  $7.9\pm 3.1^\circ\text{C}/\text{sec}$ , in line with cooling rates previously reported for chondrites and chondritic impact melt breccias [6,9,10].

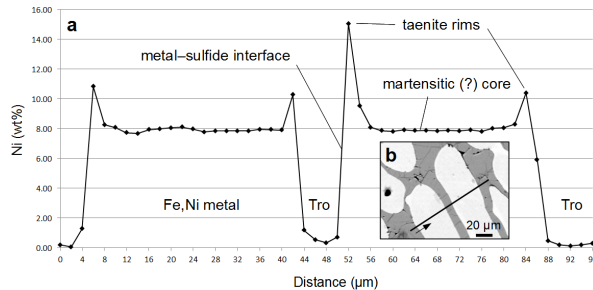


**Fig. 2:** Geochemical Ni traverse across Fe,Ni metal and sulfide in the Gao-Guenie impact melt domain. **(a)** Ni profile across two neighboring metal cells surrounded by troilite (Tro); distance between beam spots is 2  $\mu\text{m}$ . **(b)** Backscattered electron image of the metal cells in (a) and position of the electron beam traverse.

Subsolidus stage II cooling of an impact melt breccia can be quantified by determining the thickness of secondary kamacite rims surrounding Fe,Ni-metal (if cooling is slow enough so that kamacite can grow) [10,11], and/or by analyzing Ni rim gradients in the metal domains (i.e., as a measure of Ni diffusion and fractionation) [10,12].

A series of 20 Ni profiles across impact-melted Fe,Ni-metal cells did not reveal any resolvable kamacite rims in the GGIMB (Fig. 2a,b); i.e., kamacite overgrowths are either very thin ( $\leq 1 \mu\text{m}$ ) or absent. Thus, the stage II cooling rate of the GGIMB could not be determined directly. However, Ni rim gradients observed in the GGIMB, with  $\sim 7.8 \text{ wt}\%$  Ni in metal cores, and  $\sim 11.7 \text{ wt}\%$  Ni in taenite rims (indicating Fe,Ni-metal crystallization between  $\sim 750^\circ\text{C}$  and  $\sim 650^\circ\text{C}$ , under P-saturated conditions [13]) resemble those in the partially impact-melted chondrite Orvinio (H6; with  $\sim 8 \text{ wt}\%$  Ni in metal cores, and  $\sim 12.5 \text{ wt}\%$  Ni in taenite rims) [14]. The cooling rate for Orvinio was previously determined by experimentally reproducing the zoning at  $\sim 15\text{--}100^\circ\text{C}/\text{day}$  [10] (equivalent to  $\sim 1.7 \times 10^{-4}$  to  $1.2 \times 10^{-3}^\circ\text{C}/\text{sec}$  or  $\sim 5,000$  to  $40,000^\circ\text{C}/\text{yr}$  [11]). Based on the similar Ni rim gradients in the GGIMB and slightly higher Ni concentrations in troilite, the GGIMB may have cooled as rapidly as (or possibly slightly faster than) Orvinio.

**Proposed Setting for the Gao-Guenie Impact Melt Breccia:** This relatively fast cooling rate implies one of three possible geologic settings. The GGIMB could represent material that was ejected from its source crater and buried by c. 1–5 m of regolith on an

H-chondrite parent body (e.g., Fig. 11 of [11]). However, Gao-Guenie is not enriched in solar noble gases [4,5] (a hallmark of regolith breccias; e.g., [15]), which seems to contradict such origin. Moreover, since most unmelted fragments of the Gao-Guenie chondrite are only locally brecciated and mildly shocked (S1–S2 [1]), it is unlikely that the GGIMB represents a sample of the uppermost (i.e., fast-cooling) melt-bearing breccia lens inside an impact crater.

Alternatively, the small fraction of Gao-Guenie specimens that are shock-melted suggests the GGIMB represents material from a melt dike injected into the floor of an impact crater, at some depth on the H-chondrite parent body. This hypothetical scenario is in accord with the petrographic characteristics of sample LPL 1055,1.

Adopting the above cooling rate as the best available estimate for stage II cooling of the GGIMB, thermal modeling can provide further theoretical constraints on the nature and size of the impact melt body on the H-chondrite parent asteroid. A simple heat transfer model [16,17] for the center of a melt dike conductively cooling from  $750^\circ\text{C}$  to  $650^\circ\text{C}$  (assuming an ‘infinite’ plane dike geometry; no effect of volatiles, porosity, jointing and latent heat; initial melt temperatures of  $2,000^\circ\text{C}$  or  $1,180^\circ\text{C}$ ; wall rock temperatures of  $-100^\circ\text{C}$  to  $0^\circ\text{C}$ ; and using a range of thermal diffusivity values for chondrites [18]) suggests that the hypothesized impact melt dike on the H-chondrite parent asteroid was probably  $\sim 0.5\text{--}5 \text{ m}$  wide.

**References:** [1] Bourot-Denise M. et al. (1998) *MAPS*, 33, A181–A182. [2] *Met. Bull. Database* (2015) Entry for Gao-Guenie, accessed 11/05/2015. [3] Swindle T. D. et al. (2009) *MAPS*, 44, 747–762. [4] Weber H. W. et al. (1983) *Z. Naturforsch.*, 38a, 267–272. [5] Herzog G. F. et al. (1997) *MAPS*, 32, 413–422. [6] Wittmann A. et al. (2010) *JGR*, 115, E07009, 22 p. [7] Stöffler D. et al. (1991) *GCA*, 55, 3,845–3,867. [8] Scott E. R. D. (1982) *GCA*, 46, 813–823. [9] Cheek L. C. and Kring D. A. (2008) LPS IXL, abstract #1169. [10] Smith B. A. and Goldstein J. I. (1977) *GCA*, 41, 1061–1072. [11] Kring D. A. et al. (1996) *JGR*, 101, E12, 29,353–29,371. [12] Taylor G. J. et al. (1979) *GCA*, 43, 323–337. [13] Hopfe W. D. and Goldstein J. I. (2001) *MAPS*, 36, 135–154. [14] Taylor G. J. and Heymann D. (1971) *JGR*, 76, 1879–1893. [15] Osawa T. and Nagao K. (2006) *Antarct. Met. Res.*, 19, 58–78. [16] Carslaw H. S. and Jaeger J. C. (1959) *Conduction of heat in solids*. Clarendon Press, Oxford, UK, 510 pp. [17] Di Toro G. and Pennacchioni G. (2004) *J. Struct. Geol.* 26, 1783–1801. [18] Szurgot M. and Wojtawicz T. W. (2011) 74<sup>th</sup> MetSoc, abstract #5036.